Effect of Al-incorporation of nanocrystalline zinc oxide thin film prepared by chemical spray Pyrolysis method

GIRJESH SINGH[*], S.B.SHRIVASTAVA, V. GANESAN[a]
School of Studies in Physics, Vikram University, Ujjain (M.P.) India- 456010
[a]UGC-DAE-Consortium for Scientific Research, Khandwa Road, Indore (M.P) India-452017

A rapid screening methodology for the development of transparent conducting oxides is presented. The effect of Al concentration on ZnO films has been studied. All films were fabricated by a homemade chemical spray pyrolysis system (CSPT). The methodology, based on a combination of X-ray Spectrograph, Atomic Force Micrographs, UV-Visible Spectrographs and four-point probe measurements, was used to map out the structural and Opto-electronic properties over a Spray Deposited ZnO:Al film. These films are found to show high crystallinity up to (1%) Al concentration and an increase of Al concentration cause a decrease in quality of films confirmed by X-ray diffraction technique leads to introduction of defects in ZnO. The minimum resistivity and maximum transparency is obtained for the sample with nominal Al concentration of 1%. The grain sizes are found to decrease with the high Al concentration confirmed by AFM images.

1. Introduction

During last decade there has been a great deal of interest in the investigation of Zinc oxide semiconducting thin films. This is because of the fact that ZnO have strong applications in optoelectronics devices owing to its direct band gap (Eg~3.3eV) at 300K. ZnO has recently found other strong applications such as fabrication of electronic devices, transparent thin film transistor, where the protective covering preventing light exposure is eliminated since ZnO based transistor are insensitive to visible light. By controlling the doping level electrical properties can be changed from insulator through n-type semiconductor to metal while maintaining optical transparency that makes it useful for transparent electrodes in flat panel displays and solar cells[1].n-type doping of ZnO is relatively easy as compare to p-type doping . Group III element like Al, Ga and In as substitutional element of Zn can be used as n-type dopants [2]. Doping with Al, Ga and In has been attempted by many groups, resulting in high quality, highly conducting n-type ZnO thin films [3-9].Among with group III element Al has been focus of the much of the work in this area because the ionic radius of Al is smaller than that of In And Ga. Aluminium doped ZnO (AZO) films show the lowest electrical resistivity and a good optical transmittance [10-12]. For example Highly conductive ZnO:Al is regarded as a possible substitute for indium tin oxide (ITO) as an electrode materials in displays. By substitution a fraction of the Zn^{+2} ions by Al^{+3} ions, which serve as electron donor, ZnO is turns in to n-type semiconductor. Several authors [13-15] have studied the effect of Al doping on the structural, electrical and optical properties of ZnO (AZO) thin film prepared by numerous deposition techniques, such as, chemical vapour deposition (CVD) [16], radio frequency magnetron sputtering [17], sol gel process [18], pulsed laser deposition [19], electro deposition [20] and spray Pyrolysis [21, 22]. Among all of these techniques chemical spray Pyrolysis technique (CSPT) has many advantages: it is easy, inexpensive, and well adapted for mass fabrication. In this paper, we report the effect of Aluminium doping concentration on the structural, morphological, electrical and optical properties of AZO thin films deposited onto glass substrate by CSPT.

2. Experimental details

Undoped ZnO and AZO thin film at various dopants percentages were deposited by chemical spray pyrolysis technique (CSPT). Details of the deposition system and method are described B.Godbole et.al. [23].This technique is most common for the deposition of oxide thin films. Aqueous solution of Zn $(NO_3)_2.6H_2O$ was used for spraying. The doping was achieved by the addition of Al $(NO_3)_3.9H_2O$ to the precursor solution, and the whole mixture was sprayed on to the microscopic glass slides. The doping is varied in weight percentage. The concentration of Al was varied at 0.5%, 1%, 3% and 5% in the initial solution. Dry air was used as a carrier gas and the spray rate of the solution was 1cc/min. The temperature of the substrate was maintained at $380^0C\pm5^0C$ and monitored by a chromel-alumel thermocouple close to the substrates. All deposition parameters were optimized. The characterization of the prepared film was carried out by Rigaku X-ray diffractometer using Cu-Kα radiation having wavelength 1.5418 A^0, Micro-Raman spectra of the films are recorded using Labram-HR 800 spectrometer using laser radiation at wavelength of 488 nm from an Ar+ laser. Spectra are acquired by 1800 grids/mm grating, a

super-notch filter having a cut off at 100 cm^{-1} and a Peltier cooled CCD camera, allowing a spectral resolution of about 1 cm^{-1}. Laser radiation of power 10 mW is focused on to a spot of 1 μm size during Raman measurement for all the samples. The morphological studies have been done by using AFM (Digital instruments Nanoscope-IV, with Si3N4 100 mm cantilever, 0.58 N/m force constant) measurements in contact mode. The resistivity measurements were done using Keithley 617 programmable electrometer in association with Lakeshore temperature controller in a homemade set-up with Teflon insulated shielded coaxial cables. The optical measurements are done by means of UV–vis spectroscopy (PerkinElmer Lambda 950).

3. Results and discussion

3.1 Structural studies

The results of X-ray diffraction pattern of undoped ZnO and AZO films deposited at 380◦C on glass substrates for different doping concentration are shown in Fig. (1). Undoped ZnO film shows a preferential orientation along the (002) plane at 2θ=34.3^0. All Al doped films are also found to be polycrystalline with a hexagonal wurtzite-type structure. No phase corresponding to aluminium/aluminium oxide or other aluminium compound was detected in the XRD patterns. This reveals the existence of a single-phase ZnO. The preferential orientation of all films is found to be along (0 0 2) crystal plane.
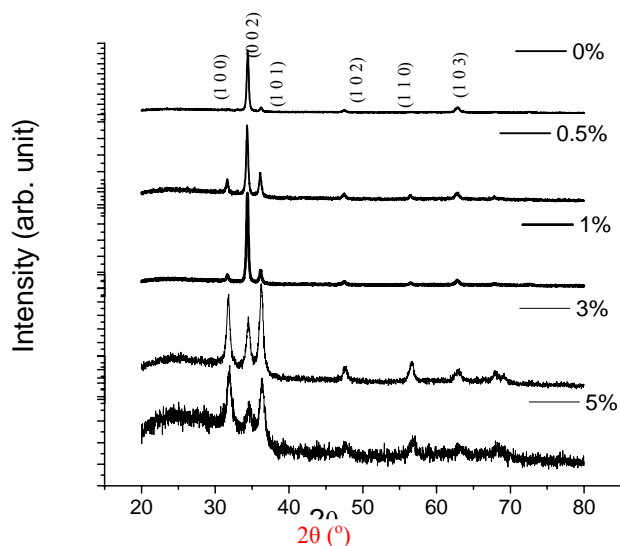

Fig. 1. XRD spectra of undoped ZnO and AZO film deposited on glass substrate at 380°C for various Al Doping concentrations.

The other peaks observed in the X-ray diffractograms of AZO films were (1 0 2), (1 1 0) and (1 0 3) but intensity of those peaks are found to be very less as compared to the preferentially oriented peaks [24]. For Al doped samples, films are polycrystalline showing a preferential orientation along (0 0 2) direction to be the most prominent for film prepared with 1% of Al dopant. However, for higher Al concentration at 3%, the intensity of (1 0 1) and (1 0 0) orientation becomes comparable to (0 0 2) orientation. This is further continuing up to 5% of Al doping, which indicates that Al doping causes a decrease of the crystalline quality of the films or introduction of defects in ZnO crystals. However thermodynamic data show that the free energy of the formation of Al_2O_3 is lower than that of ZnO, suggesting that Al_2O_3 has very high reactivity with oxygen. When Al atoms form Al_2O_3, they can not substitute Zn sites but exist as in an oxide form at grain boundaries and acting as defects. Since the orientation varies from strongly oriented growth for less doped film and finally to less oriented and poor crystallinity at highly (~5%) doped film. A similar behavior is observed for fluorine doped zinc oxide thin films [25] and aluminum doping on zinc oxide thin films grown by pulsed laser deposition technique [26]. This decrease in crystal quality may also be due to the appearance of stress because of the Difference in ion size between Zn (rZn^{2+} = 0.074 nm) and Al (rAl^{3+} = 0.054 nm) [27]. The results allow us to say that there is a predominant growth of ZnO nanocrysal with the c-axis tilted around 58 degree towards the plane of the substrate at higher doping percentage while for the sample with lower doping the c-axis is perpendicular to the plan of the substrate. This has a profound effect of corresponding Raman spectra, which indicates changes in the lattice symmetry and loss of crystalline quality in accordance with X-ray results (Fig. 7). The value of lattice constant 'C' listed in Table (1).

3.2 Morphological studies

Two-dimension surface morphology of Al doped ZnO thin film has been investigated by using atomic force micrograph. Fig. 2 (A-E) shows the (1x1 μm^2) 2D images of undoped and AZO film deposited at substrate temperature 380^{0}C. From the micrograph one can see that the total coverage of the substrate has the smooth and dense surface structure composed with uniform spherical grains. The surface analysis of 2D micrograph (1x1 μm^2) showed that the root mean square (rms) roughness and grain size of the AZO film is decreases as the Al% doping increases, which are shown in Table (1), providing large number of grain boundaries. Such type of films are useful for many applications related with surface such as gas sensor, since it can offer more surface area to interact with gas and dye molecules
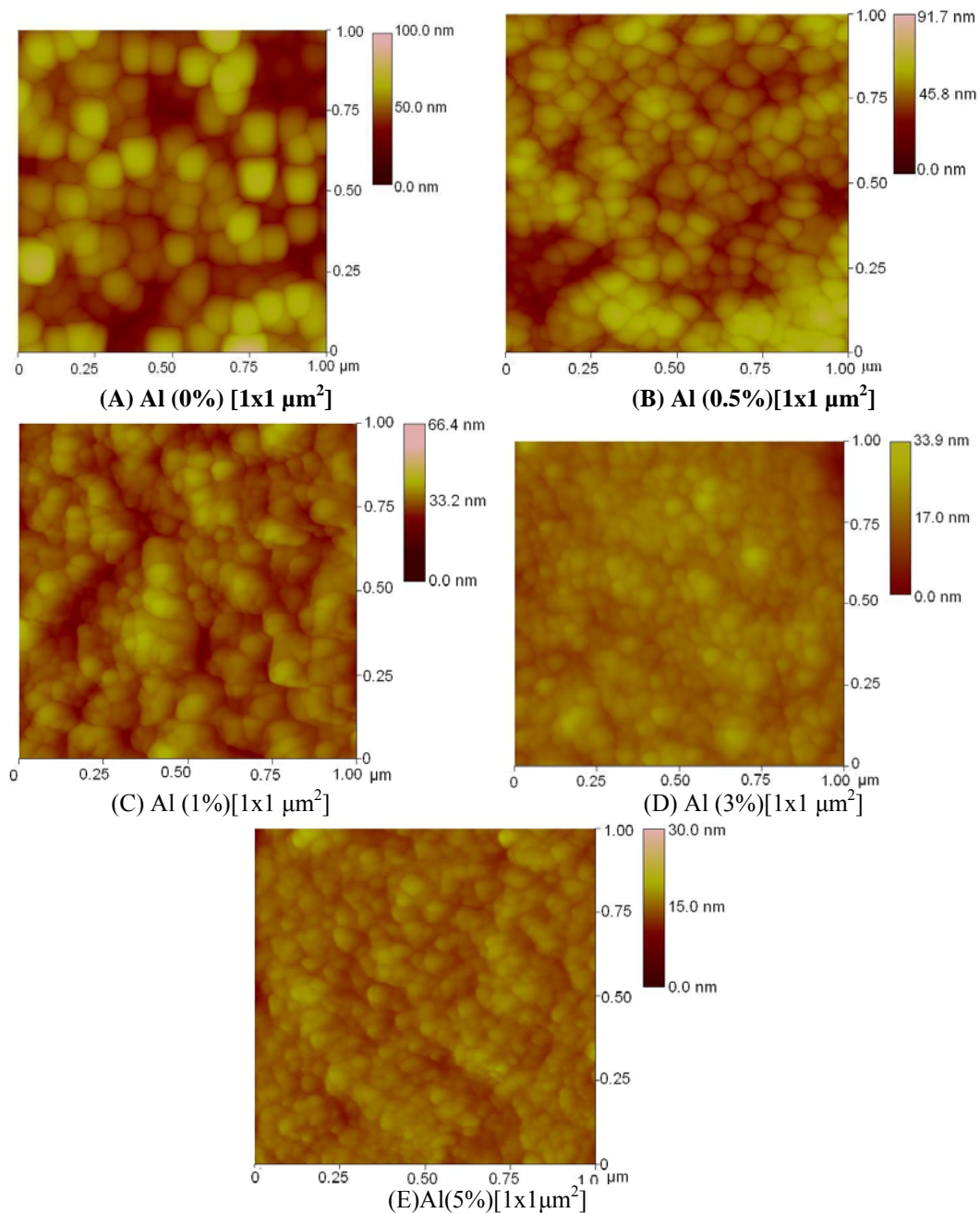
(A) Al (0%) [1x1 μm^2]

(B) Al (0.5%)[1x1 μm^2]

(C) Al (1%)[1x1 μm^2]

(D) Al (3%)[1x1 μm^2]

(E)Al(5%)[1x1μm^2]

Fig. 2. Two dimensional atomic force micrograph of AZO film at various Al concentration: (a) O% (b) 0.5% (C) 1%
(D) 3% (E) 5%

3. 3 Optical studies

Fig.3 (a) shows Transmittance Vs wavelength spectra of AZO thin film in the visible range up to 3.5 eV respectively, prepared at substrate temperature 380^{0}C, for different aluminium doping concentrations. The optical transmittance is found to increases at lower Al doping concentrations i.e. 0.5% and 1% while at higher doping it decreases. However, aluminum divided into two classes in the thin films (Al$_{Zn}$ and Al$_{Boundary}$). For thin films, Al$_{Zn}$ in the doping aluminum might be attributed to the effect of the free-carrier concentration. This decrease in transmittance at higher doping levels (>1%) may be attributed to the increase in scattering of photons by crystal defects created by doping. The free carrier absorption of photons may also be contributes to the observed reduction in optical transmittance of heavily doped film (>1%) [28]. The optical band gap (Eg) of the thin films could be obtained by plotting (αhν)^2 vs. hν curve α is the absorption coefficient and hν is the photon energy) and extrapolating the straight-line portion of this plot to the energy axis shown in Fig.3 (b). The absorption coefficient "α" has been calculated using Lambert's law for directly allowed transition for simple parabolic scheme can be described as a function of incident photon energy as [29]:

$$\alpha h\upsilon \quad \propto \quad (h\upsilon - E_g)^{1/2}$$

where Eg is the optical band. The optical band gap increase from 3.08 eV to 3.22 eV with aluminium dopant concentration from 0% to 1% and then it decreases at higher doping. The change in optical band gap is shown in Table (1). Hamberg and Granqvist [30] showed that the band gap shif is the result of two competing mechanisms: a widening can be explained in terms of Burstein moss effect [31]. This implies that, at high electron concentrations, the lowest states in the conduction band are blocked, so there is an increase in the fermi level in the conduction band of semiconductors leading to the widening of the optical band gap [32]. The decreased in band gap for samples with Al concentration higher than 1% is consistent with the increase of resistivity found in the samples with higher aluminium doping percentage (>1%) is due to electron-electron and electron-impurity scattering [32-35].
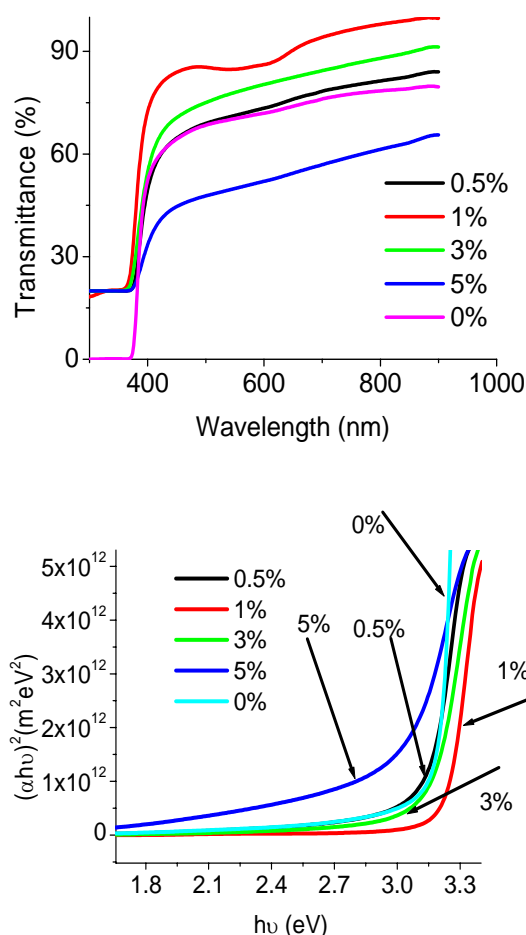
values, which varies widely with doping concentration. The absorption coefficient (α) follows an exponential law at low range of energy in accordance with Pankove's expression [37].

$$\alpha = AE_0^{\frac{3}{2}} \exp(\frac{h\upsilon}{E_0}), \quad \text{for } h\upsilon < E_g$$

Where E_0 is a parameter describing the width of the localized state in the band gap due to above mentioned effect. Semi-logarithm plots of α against photon energy (hυ) in the tail region have been shown in Fig. (4). The calculated values of the empirical parameter E_0 have also been listed in table [1].This is less for the film doped with 5% al concentration. The decrease of E_g in this case is connected with the disorder of material caused by doping. This leads to the redistribution of states from band to tail and tail to tail transition. Thus the width of tail indicates the degree of disorder in material.
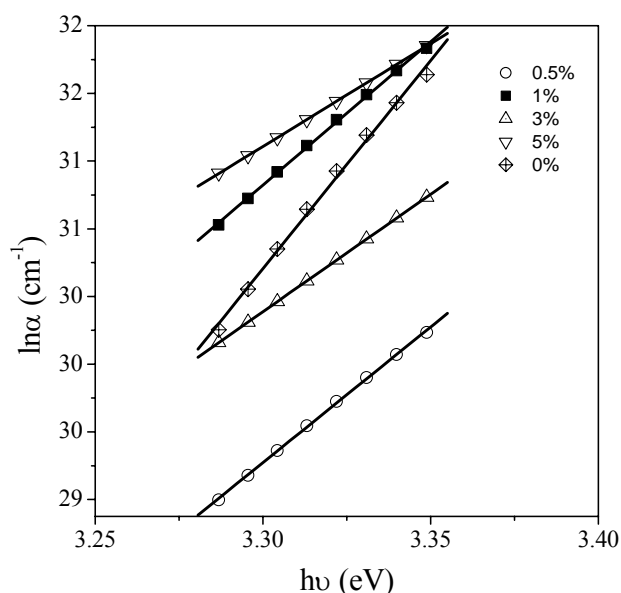

Fig.(4).Variation of ln (α) as a function of photon energy (hυ) for three dimensional ZnO thin films doped with different Al concentrations.

3.4 Electrical studies

The resistivity measurement of the above prepared films has been done by using conventional four probe resistivity method in the temperature range 150K to 350K. The results so obtained are shown in Fig.5 (a), (b), (c). From the figure it is clear that resistance decreases as the temperature increases showing the semiconducting behavior of ZnO. The activation energy (E_a) corresponding to the film prepared at various Al dopant concentrations are calculated by using Arrhenius equation

$$R_t = R_0 \exp(\frac{E_a}{K_bT})$$

where $R(t)$ is the resistivity at temperature T, K_b is the Boltzman constant. The activation energy so obtained is

Fig. 3 (a) Optical Transmittance spectra at room temprature of undoped ZnO and AZO thin film (b) (αhv)^2 vs. hv curve for undoped ZnO and AZO thin film.

The values of E_g obtained for AZO films are quite contrary to the values obtained for the different aluminum doped films prepared by sol-gel method [36]. In all those cases there was a considerable reduction in band gap

given in Table (1)**.** The electrical resistivity of AZO thin film as a function of dopant concentration is plotted in Fig.6. The minimum resistivity obtained is 0.27 (ohm-m), which is given for the sample at 1% Al doping. This decrease in resistivity is due to the increase of free carrier concentration as a results of electrons coming from the donor Al^{+3} ions incorporated as substitutional ions in Zn^{+2} cation sites or in interstitial positions creating one extra free carriers in process [38]. At higher doping concentration (>1%) the resistivity increases with Al concentration up to (~5%), this may be due to the fact that high doping concentration will lead to ionized impurity scattering from the substitutional donors and scattering from the interstitials [39].
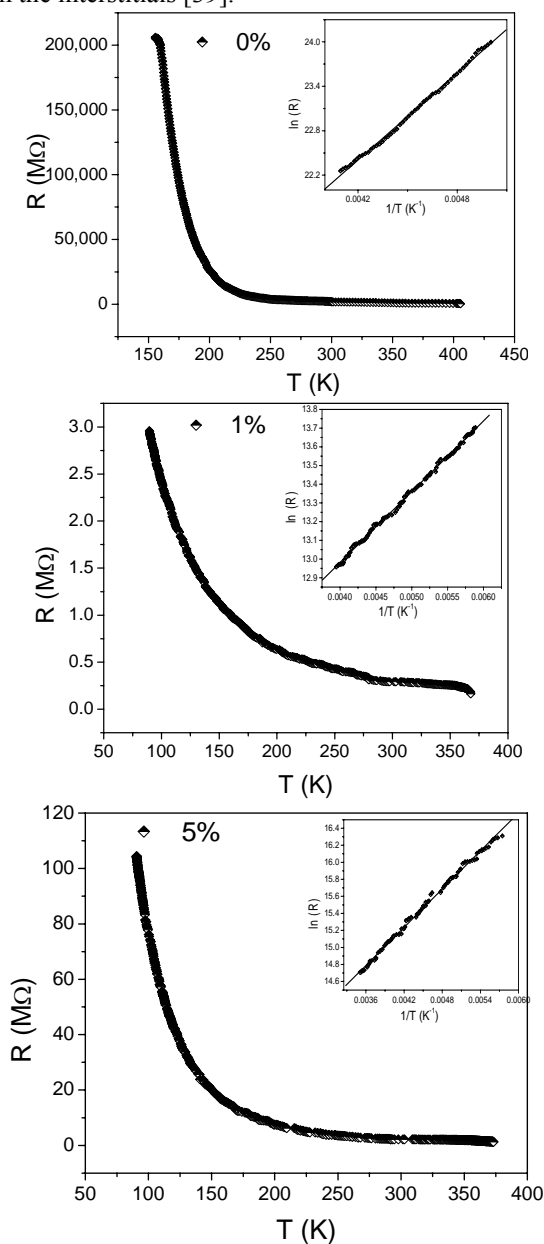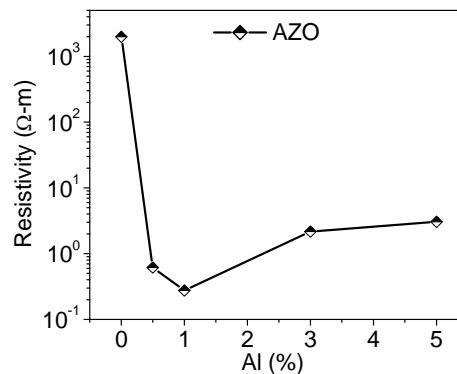

Fig.6 Electrical resistivity of undoped and AZO films deposited at 380^0C as a function of Al doping concentration.

The lack of Burstein moss effect in our highly doped samples suggests that the increase of resistivity in the doped sample above 1% Al concentration is due to a decrease in carrier concentration [40].Several authors claim that excess of Al doping for non conducting Al_2O_3 clusters in the films, causing crystal disorder and producing defects which act as a carrier traps rather than electron donors [41, 42]. However no aluminium phase is detected in X-ray deifferactogram. So it is possible that the increase of Al doping can also be cause a decrease in the crystal grain size, which is calculated by AFM data.

Fig. (7) shows the Raman scattering spectra of undoped ZnO and AZO samples. For the lattice vibration with A_1 and E_1 symmetries, the atoms move parallel and perpendicular to the c-axis respectively. The low frequency E_2 mode is associated with the vibration of the heavy Zn sublattice, while the high frequency E_2 mode involves only the oxygen atoms. In the case of highly oriented ZnO film, if the incident light exactly normal to the surface only $A_1(LO)$ and E_2 modes are observed and the other modes are forbidden according to the Raman selection rules [43].
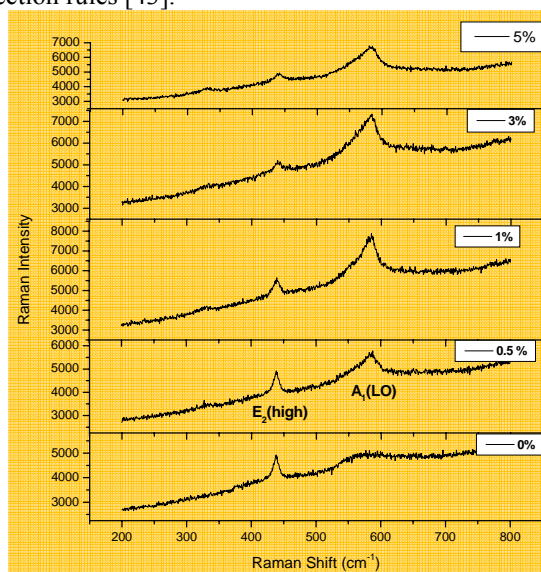

Fig. 5. Resistance vs temperature curve for Undoped and Al doped ZnO thin film at (a) 0% (b) 1% (c) 5%.

Fig.(7) Room Temprature Raman spectra of AZO film deposited on glass substrate at various Al doping concentrations.

The undoped ZnO and AZO sample shows the usual modes observed in ZnO thin film; 440cm^{-1} (E$_2$(high)), and 580 cm^{-1} (A$_1$ (LO)), this (A$_1$ (LO)) mode is hardly seen due to the weakening of LO modes by plasma phonon coupling. This effect is usual in polar semiconductors with a high free electron concentration, like ZnO and GaN [44]. As the Al doping increases in ZnO, the intensity of (E$_2$

(high)) and (A$_1$ (LO)) modes increases. While at higher doping of Al (>1%), (E$_2$ (high)) and (A$_1$ (LO)) modes decreases. This (A$_1$ (LO)) modes near 580 cm^{-1} could be observed by enhancement of Raman active and inactive phonons by the change of lattice symmetry due to disorder deactivated Raman scattering (DARS)[45].

Table-1   lattice constant, Grain size, Roughness, Optical band gap, Activation energy, and width of the localized state of the AZO films.

Al (%)	Lattice Constant "C"	Grain Size (nm)	Roughness (nm)	Optical Band Gap E$_g$ (eV)	Activation Energy (eV)	Width of localized states E$_o$ (meV)
0	5.2066	33.93	13.01	3.08	0.16	245
0.5	5.2210	30.62	7.61	3.17	0.076	160
1	5.2173	24.78	5.25	3.22	0.032	169
3	5.2266	17.73	3.01	3.12	0.035	138
5	5.2323	12.36	1.67	2.91	0.059	121

4. Conclusion

The film of Al-doped ZnO has been deposited on glass substrate by CSPT method. All films are found to be preferentially oriented along (0 0 2), although orientations are becoming lower as the Al concentration increases implies that doping with Al leads to the introduction of defects in the ZnO crystals. This has a profound effect on the corresponding Raman spectra, which indicates changes in the lattice symmetry and loss of crystalline quality in accordance with the X-ray results. The AFM micrograph reveals the cluster formation and decrease in grain size as the Al doping percentage increases. The smallest resistivity 0.27 (ohm-m) was obtained at 1% Al doping and then slightly increase at higher doping. The increase in resistivity is consistent with the decrease in band gap found in the samples with higher aluminium doping percentage (>1%) is due to electron-electron and electron-impurity scattering. So, we can say the structural, optical and electrical characteristics leads to an optimum ZnO thin film with good crystallinity.

References

[1] U. Ozgur, Ya.l.Alivov, C. Liu, A. Teke, M.K. Reshchikov, S.Dogan, V. Ayrutin, S-J. Cho, H.Morkoc, J. Applied Physics, **98**, 041301 (2005)

[2] H. Kato, M. Sano, K. Miyamoto, T. Yao, J. Cryst. Growth **237–239**, 538 (2002).

[3] S. Y. Myong, S. J. Baik, C. H. Lee, W. Y. Cho, K. S. Lim, Jpn. J. Appl. Phys., Part 2, **36**, L1078 (1997).

[4] B. M. Ataev, A. M. Bagamadova, A. M. Djabrailov, V. V. Mamedo, R. A. Rabadanov, Thin Solid Films **260**, 19 (1995).

[5] V. Assuncao, E. Fortunato, A. Marques, H. Aguas, I. Ferreira, M. E. V.Costa, R. Martins, Thin Solid Films **427,** 401 (2003).

[6] Z. F. Liu, F. K. Shan, Y. X. Li, B. C. Shin, Y. S. Yu, J. Cryst. Growth **259**, 130 (2003).

[7] M. Chen, Z. Pei, W. Xi, C. Sun, and L. Wen, Mater. Res. Soc. Symp. Proc. **666**, F.1.2 (2001).

[8] H. J. Ko, Y. F. Chen, S. K. Hong, H. Wenisch, T. Yao, D. C. Look, Appl. Phys. Lett. **77**, 3761 (2000).

[9] T. Minami, H. Nanto, S. Takata, Jpn. J. Appl. Phys., Part 2, **23**, L280 (1984).

[10] J. H. Lee, B.O. Park, Thin Solid Films **426**, 94 (2003).

[11] H. Kim, A. Pique, J.S. Horwitz, H. Murata, Z.H. Kafafi, C.M. Gilmore, D.B. Chresey, Thin Solid Films, **377–378**, 798 (2000).

[13] A. El Manouni, F.J. Manjon, M. Mollar, B.Maríb, R. Gomez, M.C. Lopez, J.R. Ramos-Barrado, Superlattices and Microstructures **39**, 185 (2006).

[14] B. Joseph, P.K.Manoj, V.K.vaidyan, Ceramic international **32**, 487 (2006).

[15] X.D. Liu, E.Y.Jiang, Solid State Communication **141**, 394 (2007) .

[16] B.M. Ataev, A.M. Bagamadova, V.V. Mamedov, A.K. Omaev, M.R. Rabadanov, J. Cryst. Growth **198–199,** 1222 (1999).

[17] D. Song, P.W. Denborg, W. Chin, A.G. Aberle, Sol. Energy Mater. Sol. Cells **73**, 1 (2002).

[18] Juarez AS, Silver AT, Ortiz A, Zironi EP, Rickards J. Thin Solid Films **333**, 196 (1998).

[19] A.V. Singh, M. Kumar, R.M. Mehra, A. Wakanaria, A. Yoshida, J. Indian. Inst. Sci. **81**, 527 (2001).

[20] J. Cembrero, A. Elmanouni, B. Hartiti, M. Mollar, B. Marí, Thin Solid Films **451–452**, 198 (2004).

[21] J.-H. Lee, B.-O. Park, Mater. Sci. Eng. B **106**, 242 (2004).

[22] J.Y. Ma, S.C. Lee, J. Mater. Sci., Mater. Electron. **11**, 35 (2000).

[23] B. Godbole, N. Badera, S. B. Shrivastava, V. Ganesan D.Jain Surface Review and Letters, **14**(6), 1 (2007).

[24] R. Brenier, L. Ortega, J. Sol–gel Sci. Technol.
29, 137 (2004).

[25] Juarez AS, Silver AT, Ortiz A, Zironi EP, Rickards J.
Thin Solid Films **333**, 196(1998).

[26] Kim H, Pique A, Horwitz JS, Murata H, Kafafi ZH,
Gilmore CM, et al. Thin Solid Films 377 (2000).

[27] A. El Manouni, F.J. Manjon, M. Mollar, B.Maríb,
R. Gomez, M.C. Lopez, J.R. Ramos-Barrado,
Superlattices and Microstructures **39**, 185 (2006).

[28] J.P. Upadhyay, S.R. Viswakarma, H.C. Prasad, Thin
Solid Films **109**, 195 (1989).

[29] A. Ables, Optical Properties of Solids, North
Holland, Amsterdam 32 (1992).

[30] I. Hamberg and C. G. Granqvist: J. Appl. Phys.
60, R123 (1986).

[31] B.E. Sernelius, K.F. Berggren, Z.C. Jin, I. Hamberg,
C.G. Granqvist, Phys. Rev. B **37**, 10244 (1998).

[32] S.H. Jeong, J.W. Lee, S.B. Lee, J.H. Boo, Thin Solid
Films **435**, 78 (2003).

[33] E. Burstain, Phys. Rev. **93**, 638 (1954).

[34] T.S. Moss, Proc. Phys. Soc. Lond.: Ser.
B **67**, 775 (1954).

[35] S.E. Sernelius, K.F. Berggren, Z.C. Jin, I. Hamberg,
C.G. Granavist, Phys. Rev. B **37**, 10244 (1988).

[36] S.Bandyopadhyay, G.K. Paul, S.K.Sen, Sol.Energy
Mater.Sol.Cell **71**(1) 103 (2001).

[37] J.I.Pankove, Phys.Rev. **140**, A2059 (1965).

[38] H. Kim, A. Pique, J.S. Horwitz, H. Murata,
Z.H. Kafafi, C.M. Gilmore, D.B.   Chresey, Thin
Solid Films **377–378** 798 (2000).

[39] W. Tang, D.C. Cameron, Thin Solid Films
238, 83 (1994).

[40] A. El Manouni, F.J. Manjon, M. Mollar, B.Mari,
R. Gomez, M.C. Lopez, J.R. Ramos-Barrado,
Ceramics International **32**, 487 (2006).

[41] J. Hu, R.G. Gordon, J. Appl. Phys. **71**, 880 (1992).

[42] A.F. Aktaruzzaman, G.L. Sharma, L.K. Malhotra,
Thin Solid Films **198**, 67 (1991).

[43] U. Ozgur, Ya.l.Alivov, C. Liu, A. Teke,
M.K. Reshchikov, S.Dogan, V. Ayrutin, S-J. Cho,
H.Morkoc, J. Applied Physics, **98**, 041301 (2005)

[44] B.H. Bairamov, A. Heinrich, G. Irmer, V.V. Toporov,
E. Ziegler, Phys. Status Solidi b **119**, 227 (1983).

[45] F.J. Manjón, B. Marí, J. Serrano, A.H. Romero,
J. Appl. Phys. **97**, 053516 (2005).

*Corresponding author: girijesh.s@gmail.com